# Generative Modelling for Phenotypic Classification

Andrea Valletta (S180768), Julia Cathrine Youngman (S123540) and Simon Daniel Eiriksson (S180722)

1 DTU Compute, Technical University of Denmark

## Introduction

Capturing variations in cellular structure is an open problem with numerous scientific applications. Generating representations of single cells that can be approximately described by a profile representing a particular population is of particular interest [Lafarge et al.]. Variational Autoencoders (VAEs) offer an efficient way of mapping complex high-dimensional data to lower dimensional representations. However, large latent spaces give rise to many latent dimensions not carrying significant information. To achieve a small and information dense latent spaces we introduce a sparsity induced prior based on the Spike and Slab distribution.

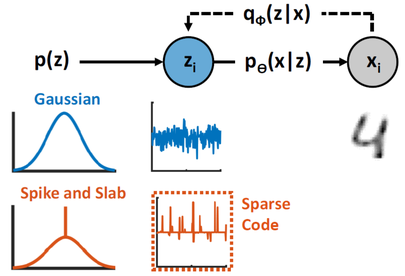


Figure 1: VAE with Gaussian vs. Spike and slab distributions as prior and their respective latent space variables. Image modified from [Tonolini et al.]

## Variational Sparse Coding

The KL-divergence consists of two terms. The first is the negative KL-divergence of the Slab variables multiplied by the probability of $z_{i,j}$ being non-zero. The second term is the negative KL divergence between the distributions of the Spike variables.

$$D_{KL}\left(q_\phi\left(z|x_i\right)||p\left(z\right)\right) = -\sum_{j}^{J}\left[\gamma_{i,j}\frac{1}{2}\left(1+\log\sigma_{z,i,j}^2-\mu_{z,i,j}^2-\sigma_{z,i,j}^2\right) - (1-\gamma_{i,j})\log\left(\frac{1-\alpha}{1-\gamma_{i,j}}\right)-\gamma_{i,j}\log\left(\frac{\alpha}{\gamma_{i,j}}\right)\right]$$

The Spike variables takes values of either 1 or zero with defined possibilities of $\alpha$ and $(1-\alpha)$, respectively. $\mu_{z,i,j}$, $\sigma_{z,i,j}$ and $\gamma_{i,j}$ are outputs of a neural network with input $x_i$.

## Experiments

The data set consists of 480,000 fluorescent microscopy images of single breast cancer cell treated for 24 hours with a collection of 113 molecules at 8 different concentrations. The cells were fixed and labelled for DNA, F-actin and B-tubulin.

For the Sparse VAE we used the images of size $\mathbf{68 \cdot 68 \times 3}$ channels as input. The final Sparse VAE used in this work was trained setting the following parameters: $\beta = \mathbf{1.0}$, $\alpha = \mathbf{0.5}$, batch size of 64 and learning rate of $\mathbf{0.001}$. Running $\mathbf{100}$ Epochs.

Profiles for each unique treatment were computed by taking the median of all wells with that specific treatment (each well was calculated as the average of all cells within the well).

A classifier using KNN=1 was built for the treatments using a hold-out method where all profiles of the same compound no matter the concentration were held out.

## Sparse VAE Learning Graphs

The training curves of the Sparse VAE of the first 100 epochs.

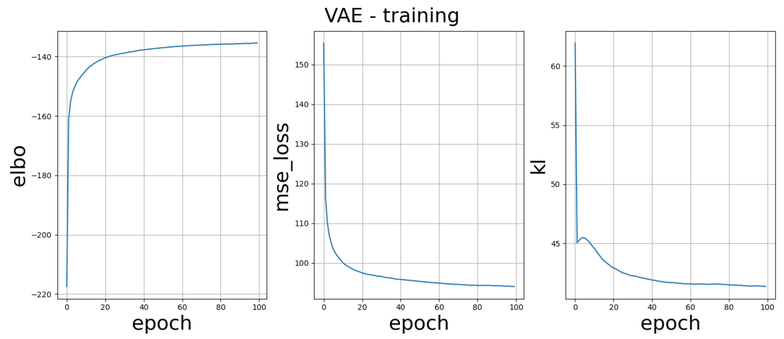


Figure 2: Training graphs for the Sparse VAE.

## Reconstructions

Below is an example of an input cell with labels (DNA, F-actin and B-tubulin) and its reconstruction in latent space.

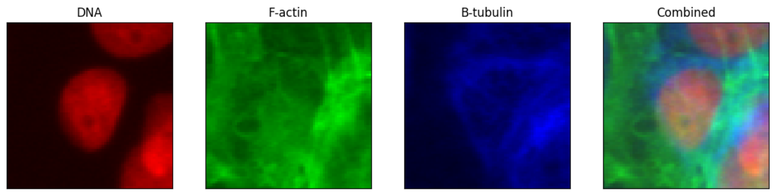


Figure 3: original image

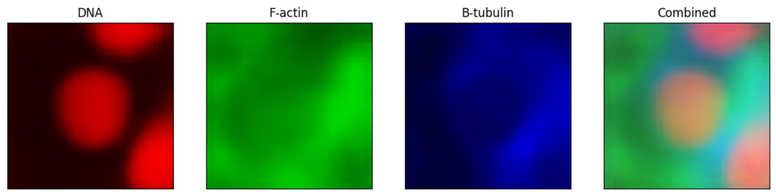


Figure 4: reconstruction

## Interpolations

The ability to interpolate between real cells from different treatment conditions and produce realistic images is powerful tool to visualize how a compound affects cellular structure. Interpolating between a control cell and a treated cell presents a hypothetical path in phenotypic space that the cell may have taken to arrive at the observed (target) state.

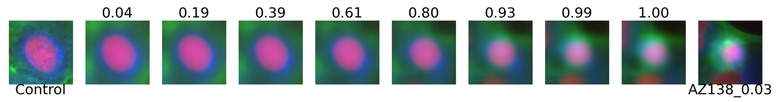


Figure 5: Translation in VAE+ latent space of a control cell (left) to a target cells (right) corresponding to compounds with different mechanisms-of-action, in this case DNA damage and microtubule stabilizer respectively. Cosine similarity between the embedding of an image and its target is shown above each interpolation.

## Heatmap

VAE Sparse model leverages on Spike and Slab distribution to find the right number of latent variables needed for: - explaining the variance in the data - reproducing the input images with the minimum loss of information. Below is the heatmap that shows the correlation between the latent variables and the labels.

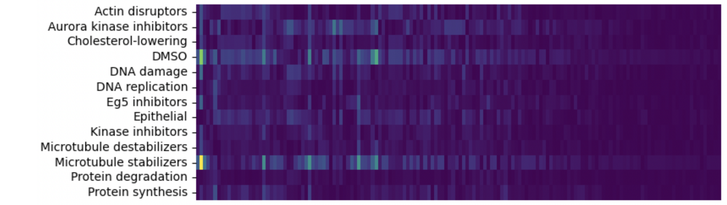


Figure 6: Heatmap of treatments vs. latent variables.

## Classifer

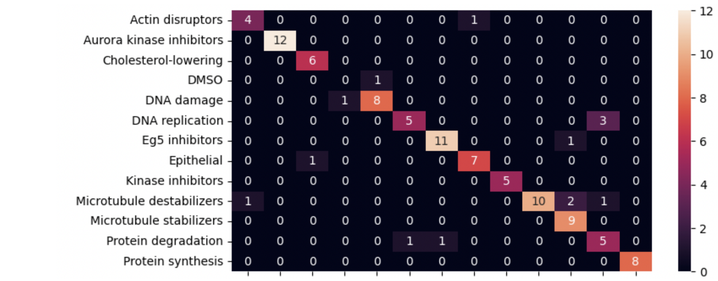


Figure 7: Confusion matrix of the predictions using the Sparse VAE model.

## Model Comparisons

The model allows for MOA classification. To train the model for classification purposes we have followed the Not-Same-Compound (NSC) used by other authors (Lafarge 2019, Ando 2017, Ljosa 2013).

Table 1: Summary of model's performance.

| | Mean | STD |
|---|---|---|
| Sparse VAE | 86.6% | - |
| Our CytoVAE | 81.73% | - |
| Lafarge VAE+ | 90.6% | 1.5% |
| Lafarge VAE | 83.5% | 1.0% |

## References

[1] Ando, Michael D., et al.: *"Improving phenotypic measurements in highcontent imaging screens"* bioRxiv, page 161422, 2017.

[2] Lafarge, Maxime W., et al: *"Capturing single-cell phenotypic variation via unsupervised representation learning"*, International Conference on Medical Imaging with Deep Learning" PMLR, 2019.

[3] Ljosa, Vebjorn, et al: *"Comparison of methods for image-based profiling of cellular morphological responses to small-molecule treatment"* J. Biomol. Screen., 18(10): 1321-1329, December 2013.

[4] Tonolini, Francesco; Jensen, Bjørn Sand and Murray-Smith, Roderick: *"Variational sparse coding"*, Uncertainty in Artificial Intelligence. PMLR, 2020.